Optical Fiber Technology 19 (2013) 109–114

Contents lists available at SciVerse ScienceDirect

Optical Fiber Technology

www.elsevier.com/locate/yofte

Regular Articles

Four-wave mixing noise in dispersion managed DWDM system including effect of randomly varying birefringence strength and orientation along fiber

Jianxin Du

College of Optoelectrical Engineering, Nanjing University of Posts & Telecommunication, Nanjing, China

ARTICLE INFO

Article history:
Received 2 July 2012
Revised 27 October 2012
Available online 27 December 2012

Keywords:
Four-wave-mixing
Dispersion maps
Dense wavelength-division-multiplexed (DWDM)
Random birefringence along fiber

ABSTRACT

Four-wave-mixing (FWM) acts as noise due to randomness of bit sequences of all channels for wavelength-division-multiplexed (DWDM) system. The approximate direct ratios of variances of FWM noise between two cases are obtained. One of them, we call "CASE A", is that the input polarization states of all channels are independently random and birefringence strength and orientation along fiber vary randomly. The other, called "CASE B", is the input polarizations of all channels are same and birefringence along the whole fiber line does not exist. Including randomness of bit sequences and walk-off between channels, for intensity-modulated/direct-detection (IM/DD) dispersion-managed (DM) DWDM system, the performance degradation due to FWM effect is calculated for "CASE A". The calculation model is based on the direct ratios between the above-mentioned two cases derived in this paper and a semi-analytic approach for "CASE B" having been introduced in previous works. The calculative results provide optimized dispersion maps used to reduce the FWM noise. In order to reduce the overall FWM noise from all channel combinations, when polarization controllers are adopted at transmitters, the launched polarizations between neighboring channels are suggested to have appropriately larger degrees of orthogonality than non-neighboring channels.

1. Introduction

There are two approaches to increase the total capacity of dense wavelength-division-multiplexed (DWDM) system. One is increasing the bit rate per channel, and the other is increasing the number of channels by incorporating narrower channel spacing. When the channel spacing becomes narrower, four-wave mixing (FWM) is dramatically elevated, potentially leading to severe degradation of system performance. It is mandatory for DWDM system designer to evaluate the degradation. As we know, the degradation depends on many factors, such as powers and chirps of signals, channel spacing, number of channels, bit patterns and rates, dispersion maps, modulation/demodulation schemes, group-velocity walk-off between channels, polarization states, nonlinear phase shifts induced by self-phase modulation (SPM) and cross-phase modulation (XPM) [1–7]. In order to accurately evaluate the degradation, the above-mentioned factors, as many as possible, should be taken into account in the process of evaluation.

For continuous-wave (CW) light, taking into account random variations of bit sequences in all channels, K. Inoue gave strict and approximate theoretical treatments to evaluate the power penalty induced by FWM effect for intensity-modulation/direct-detection (IM/DD) and frequency-shift-keying/direct-detection (FSK/DD) system [8]. For CW light as well, including the randomly varying of birefringence strength and orientation along fiber, the intensity of FWM light was approximately calculated in [9]. For return-to-zero (RZ) IM/DD DWDM system, taking into account randomness of bit sequence and group-velocity walk-off between channels, Shiva Kumar obtained analytic of power spectral density (PSD) of degenerate FWM noise for "CASE B" in [10], where the "CASE B" is that the input polarizations are identical and birefringence along fiber does not exist. For dispersion-managed (DM) RZ IM/DD DWDM system, with the method introduced by Shiva Kumar, the variance of non-degenerate FWM noise with "CASE B" was further analyzed in [11].

In this paper, we give a theoretical analysis of FWM noise for RZ DM IM/DD DWDM system with "CASE A", where the "CASE A" is that the input polarization states of all channels are independently random and birefringence strength and orientation along fiber vary randomly. The "CASE A" compared with the "CASE B" is more close to the reality of transmission fiber.

Direct ratios of variances of FWM noise between "CASE A" and "CASE B" are obtained approximately in this paper through a detailed derivation. The derivation is based on two main assumptions for simplicity of calculation. One is that the birefringence of fiber has no effect on the phase mismatch of FWM process, and the other is that the propagating matrix of light is independent of signal frequency.

E-mail address: dujx@njupt.edu.cn

1068-5200/$ - see front matter © 2012 Elsevier Inc. All rights reserved.
http://dx.doi.org/10.1016/j.yofte.2012.11.008

A parameter of FWM-induced Q-penalty (*FQP*) used to quantify the performance degradation due to FWM noise is introduced in this paper. The values of *FQP* are calculated with "CASE A" for RZ DM IM/DD DWDM system. Finally, optimized dispersion maps are suggested to reduce the effect of FWM noise. The values of Q factor including the FWM noise are analyzed for different values of average dispersion of DM fiber and the corresponding optimized dispersion maps.

The remainder of this paper is organized as follows.

In Section 2, we introduce some basic parameters and notations used through this paper. Including effect of randomly varying birefringence strength and orientation along fiber, a transfer matrix describing the evolution of light is given in Section 3. The electric-field of FWM generated in one birefringent segment is expressed in Section 4. Including effect of randomly varying birefringence strength and orientation along fiber, the variances of FWM noise for degenerate and non-degenerate conditions are analyzed in Sections 5 and 6, respectively. In Section 7, the relations between FWM noise and states of launched polarizations are analyzed. The parameter of *FQP* is defined in Section 8. For DM IM/DD DWDM system, the values of *FQP* with "CASE A" are calculated in Section 9. Conclusions are provided in Section 10.

2. Parameters and notations

In general, a practical fiber used in optical communication system can be approximately considered to be a series of many randomly oriented, linearly-birefringent fiber segments. The strength of birefringence of all segments also varies randomly along fiber. For simplicity, all the linearly-birefringent segments are assumed to be equal length. The fixed set of coordinates used in this paper is written as (x, y, z). Lights are assumed to propagate along z-axis.

The following parameters are used through this paper:

ω is the carrier frequency, α is the fiber loss, T_0 is the bit period, x is the duty cycle, k is the propagation constant, β_2 is dispersion, γ is the nonlinear coefficient, I_e is the electron current generated at detector, and P is the optical power. L is the whole fiber length. V is the group speed of pulse, $\widehat{E}$ is the vector of electric field, $\hat{e}$ is the normalized complex amplitude vector, l_e is the length of birefringent segment, N is the total number of birefringent segments.

An avalanche photodiode (APD) detector is adopted in this paper. R is a *pin* photo-detector responsivity. M is the APD current multiplication factor, and δ is the APD excess noise factor.

Subscripts and superscripts used in this paper are listed as follows:

$\tilde{n}$	integer, indicating the nth bit in bit sequence
$i = l, j, k$ *or* m subscript	the ith channel
$\exists n$ subscript	expressed in the principal axis coordinates of the nth birefringent segment. In this paper, without the notation, lights are supposed to be expressed in the fixed set of coordinates
n superscript	light is transmitting in the nth birefringent segment
$n-in$ superscript	values of quantities are given at the beginning of the nth birefringent segment
$n-out$ superscript	at the end of the nth birefringent segment
$\hat{n}$ superscript	integer, indicating that the FWM light is generated in the nth birefringent fiber segment
De subscript	the degenerate FWM condition, $\omega_{(l)} = 2\omega_{(j)} - \omega_{(m)}$
NDe subscript	the degenerate FWM condition, $\omega_{(l)} = \omega_{(j)} + \omega_{(k)} - \omega_{(m)}$
$\xi = p$ or q subscript	component of electrical field corresponding to ξ principal axis

Mathematical notations for statistical quantities are listed as follows:

$\langle\,\rangle_S$	statistical average over S, a combination of random variables, which include random bit sequences and initial phases of fields in interacting channels
$\langle\,\rangle_{S,\hat{e}}$	statistical average over S and random initial polarizations in channels

To get compact expressions, we further define:

$\widehat{E}^{(n)}_{(\exists n)}$ is $\widehat{E}_{(-n)}$, $\widehat{E}^{(\hat{n},n)}_{(\exists n)}$ is $\widehat{E}_{(+n)}$, $\widehat{E}_{(+n)(De)}$ is $\widehat{E}_{(\oplus n)}$, $\widehat{E}_{(\exists n)\xi}$ is $\widehat{E}_{(n\xi)}$ and $\widehat{E}_{(+n)(NDe)}$ is $\widehat{E}_{(\otimes n)}$.

Physical meaning of variables can be inferred from their notations listed above. For example, in the nth principal axis coordinates, the electrical field of non-degenerate FWM light generated and propagating in the nth fiber birefringent segment is written as $\widehat{E}_{(\otimes n)}$.

3. Propagating matrix including effect of randomly varying birefringence strength and orientation along fiber

According to the introduced notations in Section 2, the electric field of light, propagating in the nth birefringent segment and expressed in the nth principal axis coordinates, is written as $\widehat{E}_{(-n)}$. The following expression is obtained:

$$\begin{bmatrix} E_{(-n)p}(t,z) \\ E_{(-n)q}(t,z) \end{bmatrix} = \widehat{U}(t,z)\left[M_0^{(n)}(z)\right]\hat{e}^{(n\text{-}in)}\exp(-i\omega t) \tag{1}$$

where

$$\widehat{U}^{(n)}(t,z) = \sqrt{P_{\max}^{(n\text{-}in)}}\sum_{\tilde{n}=-\infty}^{\infty}(\overline{U}+u_{\tilde{n}})f\left(t-\tilde{n}T_0-\frac{z}{V}-\tau^{(n-in)}\right)\exp\left(-\frac{1}{2}\alpha z\right) \tag{2a}$$

$$\overline{U} = \frac{1}{2};\quad u_{\tilde{n}} = \pm\frac{1}{2} \tag{2b}$$

$$f(t) = \begin{cases} 1 & |t| < \frac{xT_0}{2} \\ 0 & \text{otherwise} \end{cases} \tag{2c}$$

$$M_0^{(n)}(z) = \begin{bmatrix} \exp(ik_p z) & 0 \\ 0 & \exp(ik_q z) \end{bmatrix}\begin{bmatrix} \cos(\psi^{(n)}) & \sin(\psi^{(n)}) \\ -\sin(\psi^{(n)}) & \cos(\psi^{(n)}) \end{bmatrix} \tag{2d}$$

where z is the distance from the beginning of the nth birefringent segment. $P_{\max}(z)$ is the peak power, $f(t, z)$ is the normalized shape function. τ is the initial time delay of bit sequence, x is duty cycle, $\psi^{(n)}$ is the anticlockwise angle between the fast direction of the n-th birefringent segment and the$x$direction of the fixed coordinates.

The optical matrix of transmission from the beginning of Ith to the end of Jth birefringent segment is written as $\Pi^{J\leftarrow I}$. The following expression is obtained

$$\Pi^{J\leftarrow I} = M^{(J)}M^{(J-1)}\cdots M^{(I)} \tag{3}$$

where

$$M^{(n)} = R^{(n\text{-}out)} M_0^{(n)}(l_e) \quad n = I, I+1, \ldots J \tag{4a}$$

$$R^{(n\text{-}out)} = \begin{bmatrix} \cos(\psi^{(n)}) & -\sin(\psi^{(n)}) \\ \sin(\psi^{(n)}) & \cos(\psi^{(n)}) \end{bmatrix} \tag{4b}$$

For simplicity, we assume $\Pi^{J \leftarrow I}$ is independent of frequency of light, thus

$$\Pi_{(i)}^{J \leftarrow I} = \Pi_{(j)}^{J \leftarrow I} \tag{5}$$

4. Electric-field due to FWM effect in one birefringent segment

Using the notations in the Section 2, in the nth principal axis coordinates, the electrical fields of FWM light generated and propagating in the nth birefringent segment, is written as $\widehat{E}_{(+n)}$. The following expression is obtained

$$\widehat{E}_{(+n)}(t,z) = \begin{bmatrix} E_{(+n)p}(t,z) \\ E_{(+n)q}(t,z) \end{bmatrix} \tag{6}$$

$$E_{(+n)\xi}(t,z) = A_{(+n)\xi}(t,z) \exp\left(i\theta_{(+n)\xi}^{(n\text{-}in)}\right) \times \exp\left\{-i[\omega t - k_{(+n)\xi} z]\right\} \quad (\xi = p \text{ or } q) \tag{7}$$

where $A_{(+n)\xi}(t,z)$ is the slowly varying envelope, $\theta_{(+n)\xi}^{(n\text{-}in)}$ is the phase at the beginning of nth birefringent fiber, and $k_{(+n)\xi}$ is the propagation constant of $E_{(+n)\xi}$.

At the end of the whole fiber link, the following expression is obtained as

$$\widehat{E}^{(\widehat{n},N\text{-}out)} = \Pi^{N \leftarrow (n+1)} \times R^{(n\text{-}out)} \widehat{E}_{(+n)}(t, L_e) \tag{8}$$

The meaning of $\widehat{E}_{(+n)}(t, L_e)$ is the corresponding electrical field of FWM light at the end of the nth birefringent fiber segment. $\widehat{E}^{(\widehat{n},N\text{-}out)}$ is the corresponding electrical field of FWM light at the end of the whole fiber. The propagation characteristic from $\widehat{E}_{(+n)}(t, L_e)$ to $\widehat{E}^{(\widehat{n},N\text{-}out)}$ is represented by the two matrices in the equation (8).

5. Variance of degenerate FWM noise including effect of randomly varying birefringence strength and orientation along fiber

According to the notations introduced in the Section 2, expressed in the nth principal axis coordinates, the electrical fields of degenerate FWM light, generated in the nth birefringent segment and propagating in it, is written as $E_{(\oplus n)}$.

The evolution of the slowly varying envelope $A_{(\oplus n)p}(t,z)$ is given by

$$\begin{aligned} \frac{\partial A_{(\oplus n)p}(t,z)}{\partial z} + \frac{\alpha}{2} A_{(\oplus n)p}(t,z) &= \exp\left(-i\theta_{(\oplus n)p}^{(n\text{-}in)}\right) \left\{ \Lambda_{1ppp^*} + \frac{2}{3} \Lambda_{1pqq^*} \exp[i\Phi(z)] \right\} \Gamma_1 \\ &\approx \frac{2}{3} \exp\left(-i\theta_{(\oplus n)p}^{(n\text{-}in)}\right) \left\{ \Lambda_{1ppp^*} + \Lambda_{1pqq^*} \exp[i\Phi(z)] \right\} \Gamma_1 \end{aligned} \tag{9}$$

where

$$\Gamma_1 = i\gamma \left(\widehat{U}_{(j)}^{(n)}\right)^2 \widehat{U}_{(m)}^{(n)} \exp\left[-i\beta_2 (\omega_{(m)} - \omega_{(j)})^2 z\right] \tag{10a}$$

$$\Lambda_{1ppp^*} = \left(e_{(j)(np)}^{(n\text{-}in)}\right)^2 \left(e_{(m)(np)}^{(n\text{-}in)}\right)^* \tag{10b}$$

$$\Lambda_{1pqq^*} = e_{(j)(np)}^{(n\text{-}in)} e_{(j)(nq)}^{(n\text{-}in)} \left(e_{(m)(nq)}^{(n\text{-}in)}\right)^* \tag{10c}$$

$$\Phi(z) = \frac{\Delta \mathrm{n}}{\mathrm{c}} (\omega_{(j)} - \omega_{(m)}) z \tag{10d}$$

The birefringence strength of Δn is about 10^{-6}–10^{-7}. In order to simplify the calculations, the value of Δn in (10d) is supposed to be zero. It indicates that birefringence of each fiber segment has no effect on the phase mismatch of FWM process. Same assumption has been given and generally testified by the experiment in the previous work [9].

The following relation is obtained approximately as

$$\begin{aligned} A_{(\oplus n)p}(t, L_e) = \frac{2}{3} \exp\left(-i\theta_{(\oplus n)p}^{(n\text{-}in)}\right) (\Lambda_{1ppp^*} + \Lambda_{1pqq^*}) \exp\left(-\frac{\alpha L_e}{2}\right) \\ \int_0^{L_e} \Gamma_1 \exp\left(\frac{\alpha z}{2}\right) \mathrm{d}z \end{aligned} \tag{11}$$

We can write

$$(\Lambda_{1ppp^*} + \Lambda_{1pqq^*}) = \begin{bmatrix} e_{(j)(np)}^{(n\text{-}in)} & e_{(j)(nq)}^{(n\text{-}in)} \end{bmatrix} \begin{bmatrix} \left(e_{(m)(np)}^{(n\text{-}in)}\right) \\ \left(e_{(m)(nq)}^{(n\text{-}in)}\right) \end{bmatrix}^* e_{(j)(np)}^{(n\text{-}in)} \tag{12}$$

Using Eq. (12), the following expression is obtained

$$(\Lambda_{1ppp^*} + \Lambda_{1pqq^*}) = \left[\hat{e}_{(m)}^{(1-in)}\right]^* \cdot \left[\hat{e}_{(j)}^{(1-in)}\right] e_{(j)(np)}^{(n\text{-}in)} \tag{13}$$

where the dot $\cdot$ represents the inner product of the vectors.

To get a compact expression, we define

$$\Theta_1^{(\widehat{n})} = \exp\left(-\frac{\alpha L_e}{2}\right) \int_0^{L_e} \Gamma_1 \exp\left(\frac{\alpha z}{2}\right) \mathrm{d}z \tag{14}$$

The term of $\Theta_1^{(\widehat{n})}$ is independent of the polarization state.

We thus get

$$A_{(\oplus n)p}(t, L_e) = \frac{2}{3} \exp\left(-i\theta_{(\oplus n)p}^{(n\text{-}in)}\right) \left[\hat{e}_{(m)}^{(1-in)}\right]^* \cdot \left[\hat{e}_{(j)}^{(1\text{-}in)}\right] \Theta_1^{(\widehat{n})} e_{(j)(np)}^{(n\text{-}in)} \tag{15}$$

In the same way mentioned above, the expression of $A_{(\oplus n)q}(t, L_e)$ is obtained as

$$A_{(\oplus n)q}(t, L_e) = \frac{2}{3} \exp\left(-i\theta_{(\oplus n)q}^{(n\text{-}in)}\right) \left[\hat{e}_{(m)}^{(1-in)}\right]^* \cdot \left[\hat{e}_{(j)}^{(1\text{-}in)}\right] \Theta_1^{(\widehat{n})} e_{(j)(nq)}^{(n\text{-}in)} \tag{16}$$

Using Eq. (16), the following expression is obtained in the fixed set of coordinates

$$\widehat{E}_1^{(n)}(t, L_e) = \frac{2}{3} \left[\hat{e}_{(m)}^{(1-in)}\right]^* \cdot \left[\hat{e}_{(j)}^{(1\text{-}in)}\right] \Theta_1^{(\widehat{n})} \hat{e}_{(j)}^{(n\text{-}out)} \exp[-i\omega_{(l)} t] \tag{17}$$

The physical meaning of $\widehat{E}_1^{(n)}(t, L_e)$ in (17) is the degenerate FWM electrical field generated in the nth birefringent segment, reaching to the end of the birefringent segment and expressed in the fixed set of coordinates.

Using Eq. (5), we can get

$$\widehat{E}_1^{(N\text{-}out)} = \frac{2}{3} \left[\hat{e}_{(m)}^{(1\text{-}in)}\right]^* \cdot \left[\hat{e}_{(j)}^{(1\text{-}in)}\right] \Theta_1^{(\widehat{n})} \hat{e}_{(j)}^{(N\text{-}out)} \exp[-i\omega_{(l)} t] \tag{18}$$

$\widehat{E}_1^{(N\text{-}out)}$ is the electrical field of $\widehat{E}_1^{(n)}(t, L_e)$ reaching the end of the whole fiber length.

Considering contributions from all birefringent segments, we can obtain

$$\begin{aligned} \widehat{E}_{1s}^{(N\text{-}out)} &= \sum_{\widehat{n}=1}^{N} \widehat{E}_1^{(N\text{-}out)} \\ &= \frac{2}{3} \left[\hat{e}_{(m)}^{(1\text{-}in)}\right]^* \cdot \left[\hat{e}_{(j)}^{(1\text{-}in)}\right] \hat{e}_{(j)}^{(N\text{-}out)} \exp[-i\omega_{(l)} t] \sum_{\widehat{n}=1}^{N} \Theta_1^{(\widehat{n})} \end{aligned} \tag{19}$$

The noise current due to signal-degenerate-FWM-tone beating is obtained as

$$\Delta I_{e1} = RM \left[\widehat{E}_{1s}^{(N\text{-}out)}\right]^* \cdot \left[\widehat{E}_{(l)}^{(N\text{-}out)}\right] + c.c. \tag{20}$$

where c.c. means complex conjugation.

Using Eqs. (19) and (5), the following expression is obtained

$$\Delta I_{e1} = \frac{2}{3} RM \left[\sum_{\widehat{n}=1}^{N} \Theta_1^{(\widehat{n})} \right]^* \left[\hat{e}_{(m)}^{(1\text{-}in)} \right] \cdot \left[\hat{e}_{(j)}^{(1\text{-}in)} \right]^* \left[\hat{e}_{(j)}^{(1\text{-}in)} \right]^* \cdot \left[\hat{E}_{(l)}^{(1\text{-}in)} \right] + c.c. \tag{21}$$

Taking into account the randomness of initial phases of the fields and bit sequences in the interacting channels, we can obtain the expression of variance of $\Delta I_{e(De)}$ as

$$\langle (\Delta I_{e1})^2 \rangle_S = G_1 \langle (\delta I_{e1})^2 \rangle_S \tag{22}$$

where

$$G_1 = \frac{8}{9} \left| \left(\hat{e}_{(m)}^{(1-in)} \right)^* \cdot \left(\hat{e}_{(j)}^{(1\text{-}in)} \right) \left(\hat{e}_{(l)}^{(1\text{-}in)} \right)^* \cdot \left(\hat{e}_{(j)}^{(1\text{-}in)} \right) \right|^2 \tag{23a}$$

$$(\delta I_{e1})^2 = R^2 M^2 P_{(l)(\max)}^{(N\text{-}out)} U_{(l)}^{(N)}(t, L_e) \left| \sum_{\widehat{n}=1}^{N} \Theta_1^{(\widehat{n})} \right|^2 \tag{23b}$$

The term of $(\delta I_{e1})^2$ is independent of the polarization state.

$\langle (\delta I_{e1})^2 \rangle_S$ can been solved by a semi-analytical approach introduced in [11].

From (22), the following expression is obtained

$$\langle (\Delta I_{e1})^2 \rangle_{S,\hat{e}} = \langle G_1 \rangle_{\hat{e}} \langle (\delta I_{e1})^2 \rangle_S \tag{24}$$

Using the statistical method for polarization states introduced in [9], the following expression is obtained

$$\langle G_1 \rangle_{\hat{e}} = \frac{2}{9} \tag{25}$$

Because ΔI_{e1} and δI_{e1} correspond to degenerate FWM case, they are represented by $\Delta I_{e(De)}$ and $\delta I_{e(De)}$, respectively.

It can be inferred that $\langle (\Delta I_{e(De)})^2 \rangle_{S,\hat{e}}$ and $\langle (\delta I_{e(De)})^2 \rangle_S$ correspond to "CASE A" and "CASE B", respectively.

6. Variance of non-degenerate FWM noise including effect of randomly varying birefringence strength and orientation along fiber

According to the notations introduced in the Section 2, expressed in the corresponding principal axis coordinates, the electrical field of non-degenerate FWM light, generated and propagating in the nth birefringent segment, is written as $E_{(\otimes n)}$.

The evolution of the slowly varying envelope $A_{(\otimes n)p}(t,z)$ is approximately given by

$$\frac{\partial A_{(\otimes n)p}(t,z)}{\partial z} + \frac{\alpha}{2} A_{(\otimes n)p}(t,z) = \exp\left(-i\theta_{(\otimes n)p}^{(n\text{-}in)}\right) \Gamma_2 (Par1 + Par2) \approx \frac{1}{3} \exp\left(-i\theta_{(\otimes n)p}^{(n\text{-}in)}\right) \Gamma_2 (Par3 + Par4) \tag{26}$$

where

$$\Gamma_2 = i2\gamma \widehat{U}_{(j)}^{(n)} \widehat{U}_{(k)}^{(n)} \widehat{U}_{(m)}^{(n)} \exp\{i[-\beta_2(\omega_{(m)} - \omega_{(j)})(\omega_{(m)} - \omega_{(k)})]z\} \tag{27a}$$

$$Par1 = \Lambda_{2ppp^*} + \frac{1}{3} \Lambda_{2pqq^*} \exp\left[i\frac{\Delta n}{c} (\omega_{(k)} - \omega_{(m)}) z \right] \tag{27b}$$

$$Par2 = \frac{1}{3} \Lambda_{2qpq^*} \exp\left[i\frac{\Delta n}{c} (\omega_{(j)} - \omega_{(m)}) z \right] \tag{27c}$$

$$Par3 = \Lambda_{2ppp^*} + \Lambda_{2pqq^*} \exp\left[i\frac{\Delta n}{c} (\omega_{(k)} - \omega_{(m)}) z \right] \tag{27d}$$

$$Par4 = \Lambda_{2ppp^*} + \Lambda_{2qpq^*} \exp\left[i\frac{\Delta n}{c} (\omega_{(j)} - \omega_{(m)}) z \right] \tag{27e}$$

where

$$\Lambda_{2ppp^*} = e_{(j)(np)}^{(n\text{-}in)} e_{(k)(np)}^{(n\text{-}in)} \left(e_{(m)(np)}^{(n\text{-}in)} \right)^* \tag{28a}$$

$$\Lambda_{2pqq^*} = e_{(j)(np)}^{(n\text{-}in)} e_{(k)(nq)}^{(n\text{-}in)} \left(e_{(m)(nq)}^{(n\text{-}in)} \right)^* \tag{28b}$$

$$\Lambda_{2qpq^*} = e_{(j)(nq)}^{(n\text{-}in)} e_{(k)(np)}^{(n\text{-}in)} \left(e_{(m)(nq)}^{(n\text{-}in)} \right)^* \tag{28c}$$

Similar to Eq. (10), the values of Δn in (27) is also supposed to be zero.

The solution of $A_{(\otimes n)p}(t,z)$ is approximately given by

$$A_{(\otimes n)p}(t, L_e) = \frac{1}{3} \exp(-i\theta_{(\otimes n)p}) \left[(\Lambda_{2ppp^*} + \Lambda_{2pqq^*}) + (\Lambda_{2ppp^*} + \Lambda_{2qpq^*}) \right] \times \exp\left(-\frac{\alpha L_e}{2}\right) \int_0^{L_e} \Gamma_2 \exp\left(\frac{\alpha z}{2}\right) \mathrm{d}z \tag{29}$$

Using Eq. (5), the following expression is obtained

$$\Lambda_{2ppp^*} + \Lambda_{2pqq^*} = \left[\hat{e}_{(m)}^{(1-in)} \right]^* \cdot \left[\hat{e}_{(k)}^{(1-in)} \right] e_{(j)(np)p}^{(n\text{-}in)} \tag{30a}$$

$$\Lambda_{2ppp^*} + \Lambda_{2qpq^*} = \left[\hat{e}_{(m)}^{(1\text{-}in)} \right]^* \cdot \left[\hat{e}_{(j)}^{(1\text{-}in)} \right] e_{(k)(np)}^{(n\text{-}in)} \tag{30b}$$

To get a compact expression, we define

$$\Theta_2^{(\widehat{n})} = \exp\left(-\frac{\alpha L_e}{2}\right) \int_0^{L_e} \Gamma_2 \exp\left(\frac{\alpha z}{2}\right) \mathrm{d}z \tag{31}$$

The term of $\Theta_2^{(\widehat{n})}$ is independent of the polarization state.

We thus get

$$\widehat{E}_2^{(n)}(t, L_e) = \frac{1}{3} \Theta_2^{(\widehat{n})} \exp[i\omega_{(l)} t] \left\{ \left[\hat{e}_{(m)}^{(1-in)} \right]^* \cdot \left[\hat{e}_{(k)}^{(1\text{-}in)} \right] e_{(j)}^{(n\text{-}out)} + \left[\hat{e}_{(m)}^{(1\text{-}in)} \right]^* \cdot \left[\hat{e}_{(j)}^{(1-in)} \right] \hat{e}_{(k)}^{(n\text{-}out)} \right\} \tag{32}$$

The meaning of $\widehat{E}_2^{(n)}(t, L_e)$ is the non-degenerate FWM electrical field generated in the nth birefringent segment, reaching to the end of the birefringent segment and expressed in the fixed set of coordinates.

Using the similar derivation presented in Section 5, we can obtain the expression of variance of ΔI_{e2} as

$$\langle (\Delta I_{e2})^2 \rangle_S = G_2 \langle (\delta I_{e2})^2 \rangle_S \tag{33}$$

where

$$(\delta I_{e2})^2 = R^2 M^2 P_{(l)(\max)}^{(N\text{-}out)} U_{(l)}^{(N)}(t, L_e) \left| \sum_{\widehat{n}=1}^{N} \Theta_2^{(\widehat{n})} \right|^2 \tag{34}$$

The term of $(\delta I_{e2})^2$ is independent of the polarization state.

$\langle (\delta I_{e2})^2 \rangle_S$ can been solved using the semi-analytical calculation method introduced in [11].

$$G_2 = G_{21} + G_{22} + G_{23} \tag{35}$$

where

$$G_{21} = \frac{2}{9} \left| \left(\hat{e}_{(m)}^{(1\text{-}in)} \right)^* \cdot \left(\hat{e}_{(j)}^{(1\text{-}in)} \right) \left(\hat{e}_{(l)}^{(1\text{-}in)} \right)^* \cdot \left(\hat{e}_{(k)}^{(1\text{-}in)} \right) \right|^2 \tag{36a}$$

$$G_{22} = \frac{2}{9} \left| \left(\hat{e}_{(m)}^{(1\text{-}in)} \right)^* \cdot \left(\hat{e}_{(k)}^{(1\text{-}in)} \right) \left(\hat{e}_{(l)}^{(1\text{-}in)} \right)^* \cdot \left(\hat{e}_{(j)}^{(1\text{-}in)} \right) \right|^2 \tag{36b}$$

$$G_{23} = \frac{2}{9} \left(\hat{e}_{(m)}^{(1\text{-}in)} \right)^* \cdot \left(\hat{e}_{(j)}^{(1\text{-}in)} \right) \left(\hat{e}_{(l)}^{(1\text{-}in)} \right)^* \cdot \left(\hat{e}_{(k)}^{(1\text{-}in)} \right) \left(\hat{e}_{(k)}^{(1\text{-}in)} \right)^* \cdot \left(\hat{e}_{(m)}^{(1\text{-}in)} \right) \left(\hat{e}_{(j)}^{(1\text{-}in)} \right)^* \cdot \left(\hat{e}_{(l)}^{(1\text{-}in)} \right) + c.c. \tag{36c}$$

From (33), similar to (24) and (25), the following relations are obtained

$$\langle (\Delta I_{e2})^2 \rangle_{S,\hat{e}} = \langle G_2 \rangle_{\hat{e}} \langle (\delta I_{e2})^2 \rangle_S \tag{37a}$$

$$\langle G_2 \rangle_{\hat{e}} = \frac{1}{6} \tag{37b}$$

Because ΔI_{e2} and δI_{e2} correspond to non-degenerate FWM case, they are written by $\Delta I_{e(NDe)}$ and $\delta I_{e(NDe)}$, respectively.

It can be inferred that $\langle(\Delta I_{e(NDe)})^2\rangle_{S,\hat{e}}$ and $\langle(\delta I_{e(NDe)})^2\rangle_S$ correspond to "CASE A" and "CASE B", respectively.

7. The instance that initial polarizations are controllable

It can be inferred from Eqs. (22), (23), (33)–(36) that the degree of orthogonality between the input polarizations has great impact on the FWM noise. For example, if $\hat{e}^{(1-in)}_{(m)}$ is orthogonal to $\hat{e}^{(1-in)}_{(j)}$, the value of $\langle(\Delta I_{e(De)})^2\rangle_S$ is zero. In general, narrower channel spacing, larger values of $\langle(\delta I_{e(De)})^2\rangle_S$ and $\langle(\delta I_{e(NDe)})^2\rangle_S$ are [10]. Therefore, in order to reduce the overall FWM noise, when polarization controllers are adopted at transmitters, launched polarizations between neighboring channels are suggested to have appropriately larger degrees of orthogonality than non-neighboring channels, but the obtaining optimal degrees of polarization orthogonality between the interacting channels is a time-consuming task of numerical calculations, so this paper will not include it.

8. Introduction of FWM-induced Q-factor penalty

In order to keep expressions concise, we define

$$\sigma^2_{(jkm)} = \langle(\Delta I_{e(NDe)})^2\rangle_{S,\hat{e}} \tag{38a}$$

$$\sigma^2_{(jjm)} = \langle(\Delta I_{e(De)})^2\rangle_{S,\hat{e}} \tag{38b}$$

where the subscript of (jkm) indicates the non-degenerate FWM condition $\omega_{(l)} = \omega_{(j)} + \omega_{(k)} - \omega_{(m)}$, while (jjm) indicates the degenerate FWM condition $\omega_{(l)} = 2\omega_{(j)} - \omega_{(m)}$.

Many FWM terms corresponding to different channel combinations probably fall on same detected channel. For "mark", the total variance of electron current can be approximately expressed as

$$\sigma^2_{Mark} = \sum_{j\neq k\neq m} \sigma^2_{(jkm)} + \sum_{j\neq m} \sigma^2_{(jjm)} + \sigma^2_{sx} + N_{th} + N_{sh} \tag{39}$$

where

$$\sigma^2_{sx} = 4R^2M^2P_sS_{ASE}B \tag{40a}$$

$$S_{ASE} = N_{am}h\nu n_{sp}[G-1] \tag{40b}$$

$$N_{sh} = 2eRP_sBM^2M^{\delta} \tag{40c}$$

$$N_{th} = \frac{4k_BT}{R_L}B \tag{40d}$$

where σ^2_{sx}, N_{th} and N_{sh} are the variances of signal-ASE beat, thermal and shot noises, respectively. S_{ASE} is the power spectral density of ASE noise. n_{sp} is the spontaneous emission factor, G is the amplifier gain, P_s is the power of optical signal at photodiode detector, h is Planck's constant, ν is frequency, e is electron charge, R_L is the load resistance, k_B is Boltzmann's constant, T is absolute temperature, B is the bandwidth of introduced rectangular electrical filter.

For "space", the total variance of electron current is approximately given as

$$\sigma^2_{Space} = N_{th} \tag{41}$$

For mark, the average value of electron current I_e is expressed as

$$\langle I_{e(Mark)}\rangle = RP_s \tag{42}$$

For space, $\langle I_{e(Space)}\rangle = 0$.

The Q-factor is given as

$$Q = \frac{\langle I_{e(Mark)}\rangle - \langle I_{e(Space)}\rangle}{\sigma_{Mark} + \sigma_{Space}} \tag{43}$$

Taking into account FWM effect, Q-factor is expressed as

$$Q_{tot} = \frac{RMP_s}{\sqrt{\sum_{j\neq k\neq m} \sigma^2_{(jkm)} + \sum_{j\neq m} \sigma^2_{(jjm)} + \sigma^2_{sx} + N_{th} + N_{sh}} + \sqrt{N_{th}}} \tag{44}$$

Ignoring the FWM effect, Q-factor is given as

$$Q_0 = \frac{RMP_s}{\sqrt{\sigma^2_{sx} + N_{th} + N_{sh}} + \sqrt{N_{th}}} \tag{45}$$

The parameter of *FQP* is defined as

$$FQP = 10\log(Q_0/Q_{tot}) \tag{46}$$

Larger value of *FQP* indicates more impact of FWM effect on system performance.

9. Example calculations of *FQP* with "CASE A" for DM fiber link

The transmission line in our study is assumed to be including many repeated DM units. Each unit consists of two fiber parts with the second-order dispersion parameters β_{2+} and β_{2-}, respectively as shown in Fig. 1. In the figure, β_{2av} is the average second-order dispersion in one dispersion unit. The lumped amplifiers used to completely compensate for the fiber loss have the same spacing as the dispersion period, the length of which is L. The lengths of two sections with β_{2+} and β_{2-} in one dispersion unit are L_1 and L_2, respectively.

The values of *FQP*with "CASE A" are calculated for DM IM/DD DWDM system. Our calculation model is based on the direct ratios derived above and a semi-analytic approach for "CASE B" introduced in the previous work [11]. Some parameters used in this paper are summarized in Table 1.

Other parameters are given as follows:

Initial delays of bit sequences in all channels τ_0 are supposed to be zero. Initial peak powers of pulses in all channels $P_{\max 0}$ are 5 mW. Nonlinear coefficients of two kinds of fibers assumed to be same are 2.43 $W^{-1}km^{-1}$. Spontaneous emission factor of optical amplifier $\mathbf{n}_{sp}$ is 2. Initial chirp in per channel C_0 is 0. The bandwidth of rectangular electrical filter B is supposed to be 0.5 R_b. Dispersion slope of fiber is supposed to be 0.

In order to clarify the relation between the values of *FQP* and dispersion maps, we define

$$S = \frac{\beta_{2-}L_2 - \beta_{2+}L_1}{\beta_{2av}L} \tag{47a}$$

$$\rho = \frac{L_1}{L_1 + L_2} \tag{47b}$$

where S is defined as the dispersion map strength. The calculation results are shown by Fig. 2. It can be concluded from Fig. 2 that the value of *FQP* depends more strongly on ρ when the value of S becomes smaller. A general trend also can be inferred from the figure that larger values of S correspond to smaller values of *FQP*. How-

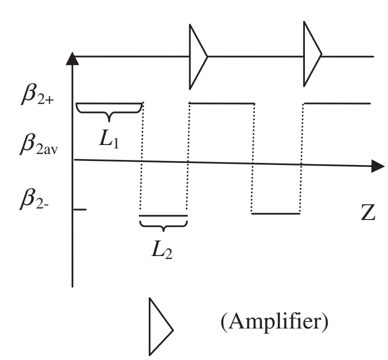

Fig. 1. Dispersion map and amplifier position.

Table 1
Some parameters for DM IM/DD DWDM system used in this paper.

Description	Symbol	Value	Description	Symbol	Value
Duty cycle of RZ modulation	x	0.5	Length of DM unit	L	50 km
Number of DM units	N_u	20	Number of channels	N_c	17
Bit rate in per channel	R_b	40 Gb/s	Wavelength spacing	$\Delta\lambda$	0.4 nm
Wavelength of central channel	λ_c	1552.52 nm	APD excess noise factor	δ	0.7
Load resistance of receiver circuit	R_L	1000 Ω	Absolute temperature of receiver	T	293 K
Current multiplication factor of APD	M	10	*pin* photo-detector responsivity	R	0.8 A/W

ever, in general, larger values of S, more dispersive waves will be emitted, as can be numerically explained by a split step Fourier method (SSFM) [12]. Therefore, it can be derived from Fig. 2 that the optimal dispersion map with $\beta_{2av} = -0.5$ ps^2/km is the combination of $S = 3$ and $\rho = 0.3$.

The optimal dispersion maps for other values of β_{2av} can be derived in a same way. Calculative results show that the optimal dispersion maps for different values of β_{2av} generally is different. With the corresponding optimal dispersion maps, the dependence of Q_{tot} on β_{2av} is shown by Fig. 3. A general trend can be inferred from Fig. 3 that larger absolute values of β_{2av} correspond to larger values of Q_{tot}.

By applying the calculation method introduced in this paper, similar analysis can be done corresponding to other modulation/detection schemes for DM DWDM system.

10. Conclusion

In this paper, we have derived a semi-analytic calculative method to quantify the degradation of performance induced by FWM effect

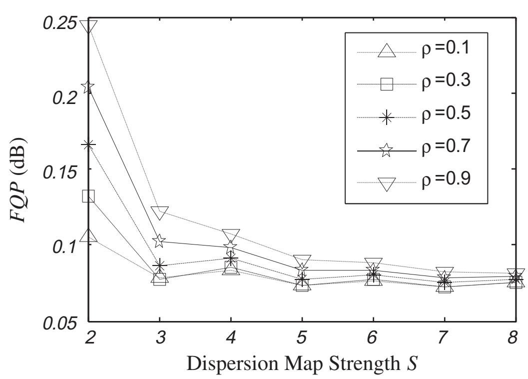

Fig. 2. *FQP* versus ρ and S with $\beta_{2av} = -0.5$ ps^2/km.

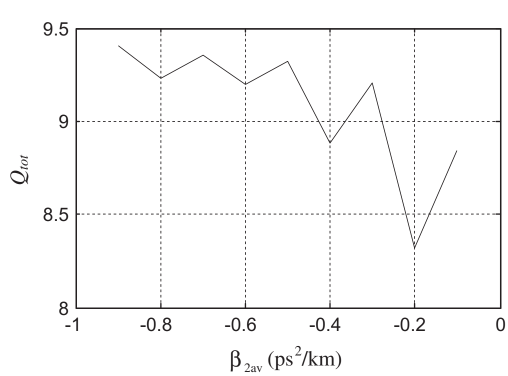

Fig. 3. Q_{tot} versus β_{2av}.

for IM/DD RZ DM DWDM system with "CASE A". The "CASE A" corresponds to birefringence strength and orientation varying randomly along fiber and random initial polarization states in all channels.

The "CASE B" is that the input polarizations of all channels are same and birefringence along the whole transmission line does not exist. The calculation method of variances of FWM noise with the "CASE B" for DM fiber link have been derived in the previous work, which had taken into account the randomness of bit sequences in all channels and walk off between channels.

The approximate direct ratios of variances of FWM noise are derived between "CASE A" and "CASE B" in this paper. On the base of the derived ratios, the calculation of variances of FWM noise with "CASE A" is given.

When polarization controllers are adopted at transmitters, launched polarizations between neighboring channels are suggested to have appropriately larger degrees of orthogonality than non-neighboring channels.

The method introduced in this paper can be applied to other modulation/detection schemes for DWDM system.

For simplicity, many factors have not been taken into account in this study, which include the varying of pulse width with distance, randomness of initial delays of bit sequences, initial chirps of signal pulses, dispersion slope, polarization-mode-dispersion (PMD), nonlinear phase shift induced by SPM and XPM, etc. which will be incorporated in a future paper.

Acknowledgments

This work was supported in part by a National Natural Science Foundation of China under Grant 61077084 and the Scientific Research Foundation of Nanjing University of Posts and Telecommunications (NY212001).

References

[1] I. Neokosmidis, T. Kamalakis, A. Chipouras, T. Sphicopoulos, IEEE J. Lightw. Technol. 23 (2005) 1137–1144.
[2] A. Bogoni, L. Potì, A. Bononi, IEEE Photon. Technol. Lett. 15 (2003) 260–262.
[3] M. Wu, W.I. Way, IEEE J. Lightw. Technol. 22 (2004) 1483–1497.
[4] S. Song, C.T. Allen, K.R. Demarest, R. Hui, IEEE J. Lightw. Technol. 17 (1999) 2285–2290.
[5] R.W. Tkach, A.R. Chraplyvy, F. Forghieri, A.H. Gnauck, R.M. Derosier, IEEE J. Lightw. Technol. 13 (1995) 841–849.
[6] K. Inoue, H. Toba, IEEE J. Lightw. Technol. 10 (1992) 361–366.
[7] K. Inoue, N. Shibata, Opt. Lett. 14 (1989) 584–586.
[8] K. Inoue, K. Nakanishi, K. Oda, H. Toba, IEEE J. Lightw. Technol. 12 (1994) 1423–1439.
[9] K. Inoue, IEEE J. Quantum Electron. 28 (1992) 883–894.
[10] S. Kumar, IEEE J. Lightw. Technol. 23 (2005) 310–320.
[11] J. Du, Opt. Commun. 282 (2009) 2983–2989.
[12] O.V. Sinkin, R. Holzlöhner, J. Zweck, C.R. Menyuk, IEEE J. Lightw. Technol. 21 (2003) 61–67.